P. LACKI*, K. ADAMUS*, K. WOJSYK*, M. ZAWADZKI**, Z. NITKIEWICZ*

MODELING OF HEAT SOURCE BASED ON PARAMETERS OF ELECTRON BEAM WELDING PROCESS

MODELOWANIE ŹRÓDŁA CIEPŁA NA PODSTAWIE PARAMETRÓW PROCESU SPAWANIA WIĄZKĄ ELEKTRONÓW

In the paper thermo-mechanical analysis of Inconel 706 tube welding process was presented. Tubes were joined using electron beam welding EBW. Process simulation was performed using finite element method, FEM Key aspect of welding process simulation is definition of heat source. Geometry of heat source and heat input have direct impact on fusion zone, FZ, and heat affected zone, HAZ. The goal of the work was to design EBW that will produce FZ of required depth. The set of process parameters was identified based on work of Ferro for Inconel 706. Modification of the process parameters was required. For this purpose partial least square method, PLS, was used. PLS model was built using results of own work on EBW for 18-8 steel. The model was applied to Inconel data. The results calculated by PLS model were used to build FEM model.

Keywords: electron beam welding, partial least squares, finite element method

W pracy przedstawiono analizę termo-mechaniczną procesu spawania tulei wykonanych ze stopu Inconel 706. Tuleje połączono za pomocą wiązki elektronów. Symulacja procesu została wykonana przy użyciu metody elementów skończonych, MES. Kluczowym aspektem przy symulacji procesu spawania jest zdefiniowanie źródła ciepła. Geometria źródła ciepła i ilość wydzielonej mocy mają bezpośredni wpływ na strefę przetopienia i strefę wpływu ciepła. Celem pracy jest zaprojektowanie procesu spawania wiązką elektronów w celu uzyskania określonej głębokości spoiny. Zestaw parametrów procesu spawania został określony na podstawie pracy Ferro wykonanej dla stopu Inconel 706. Wymagana była modyfikacja parametrów przedstawionych w pracy. W tym celu wykorzystano metodę częściowo najmniejszych kwadratów, PLS. Model PLS został zbudowany na podstawie wyników badań własnych dla spawania stali 18-8 za pomocą wiązki elektronów. Opracowany model został wykorzystany do modyfikacji parametrów spawania. Otrzymane wyniki posłużyły do opracowania modelu MES procesu spawania.

1. Electron beam welding

EBW is fusion welding technology. It is described in [1] and [2]. Distinct features of EBW are high power density (10^7 W/cm^2) combined with beam power in the range from 0.5kW to 300kW. Wide range of beams powers allows for joining elements with thickness from 0.2mm to 300mm. High power density enables creating welds with comparatively small fusion zone and heat affected zone. Thus small distortions are introduced during welding.

Unlike in case of electric arc welding heat is produced inside material and is not transferred through external layer. Heat generation process follows from the fact that electrons have the capability of penetrating through material. At accelerating voltage of 150 kV electrons penetrate at depth of 0.06mm. Upon electron penetration and collision their kinetic energy is converted into heat. Depending on the beam power density EB unit can operate in either shallow or deep penetration mode.

At power densities above $0.5 \cdot 10^5$W/cm^2 at small depth mentioned the energy is produced at such high rate that the surrounding material is unable to transfer it further using conduction. Thus material is first melted and subsequently vaporized. The vapor presses liquid downwards and sideways. As a result depression forms It allows beam to access deeper material layers. As the process continues deep thin canal called keyhole is created. At sufficient beam powers keyhole allows electron beam to penetrate through the whole thickness of material. As the beam moves along welding trajectory molten material replaces keyhole and solidifies to produce final

* CZĘSTOCHOWA UNIVERSITY OF TECHNOLOGY, INSTITUTE OF METAL FORMING, QUALITY ENGINEERING AND BIOENGINEERING, 42-200 CZĘSTOCHOWA, 21 ARMII KRAJOWEJ AV., POLAND
** WSK "PZL-RZESZÓW" S.A., 35-078 RZESZÓW, 120 HETMAŃSKA STR., POLAND

weld. In deep penetration mode the maximal ratio of width to depth can achieve values ranging from 1:10 to 1:50.

At low beam power densities EB unit operates in shallow penetration mode. Weld pool has the shape characteristic for arc welding processes. Fusion zone is wide and shallow.

EB is produced by heating cathode made of high melting point metals such as tungsten or tantalum. At high temperature electrons detach from cathode and gather around it In order to accelerate electrons and direct them toward welded workpiece electric field is created. Negative voltage is applied to cathode and anode is set to earth potential. Thus electrons flow from cathode through ring shaped anode toward workpiece. EB passing through anode has final velocity but it doesn't have the required power density. In order to achieve high density power beam passes through annular coil that produces magnetic field which focuses electrons. EB of diameter in the range 0.11.0mm can be produced. The highest penetration depth is achieved for beam that is focused on the surface of workpiece.

EBW is performed in vacuum. There are two reasons for this. In atmosphere electrons forming beam would collide with heavier gas particles which would cause beam defocus and loss of power density. Additionally air ionization would occur which would cause destruction of cathode. Generation of vacuum requires application of vacuum chamber which is the main drawback of EBW technology. The welded objects must fit into the chamber. Also significant time is needed to empty the chamber. The advantage of using vacuum is the capability of welding materials that easily react with atmospheric gases, for instance, titanium.

2. Inconel 706

Inconel 706 is nickel-iron-chromium alloy that is characterized by high mechanical strength. Its properties are described in [3]. For cold-rolled sheet yield strength is 383MPa and tensile strength is 757MPa. Melting point ranges from 1334 to 1371°C. The distinct feature of Inconel 706 is that is maintains high strength and offers high corrosion resistance at high temperatures. For these reasons it is applied in aerospace industry for components that operate at high temperatures: cases, shafts and discs of turbines, diffusers, compressors. In these applications joining of elements using welding is required. Inconel 706 was based on Inconel 718 and similar welding procedures apply. EBW is preferred technology for joining Inconel alloy parts. It offers high power density and allows for joining of thick sections with very low heat input. Low heat input produces small HAZ and FZ,

and introduces relatively small distortions and thermal stresses which are one of the factors causing hot cracking phenomena during welding processes [4, 5]. Additionally low heat input minimizes Nb segregation and Laves formation which are undesirable phenomena as they increase Inconel 718 brittleness [6].

3. EBW process design

The purpose of EBW process is to join 2 tubes made of Inconel 706 alloy. Tubes' diameter is 32.5 mm. One tube has walls 4.5 mm thick and the other has walls 5.5 mm thick. The thicker tube has welding collar which facilitates fitting tubes together. The length of each of tubes is 50 mm. It was assumed that fusion zone should have depth of 5mm. EBW process design consist in identification of the set of parameters that will produce weld of the required depth.

The basis for process design will be results Ferro's work [5] on impact of electron beam welding process parameters on geometry of FZ for Inconel 706 Since the results don't contain the set of parameters for the target depth of 5mm the modification of the described set of parameters was required. For this purpose Partial Least Square, PLS, method was be applied. Sample application of PLS in welding domain was described by Yang et al [7].

The data from own research describing dependency between FZ geometry and welding process parameters were used to build PLS model. The data were obtained for EBW process of 18-8 steel plates. Subsequently PLS model was applied to the set of parameters for Inconel. It provided information about the changes necessary to produce depth to 5mm.

4. Partial least square method

PLS method similarly to ordinary least squares, OLS, method optimizes parameters of model equations that define dependency between explanatory and response variables. Optimization is performed with respect to minimization of errors between actual values and values predicted by model. The main difference is that PLS, unlike OLS, operates on hidden variables also called latent variables. Hidden variables are linear combination of original variables. Hidden variable extraction is performed one by one.

The first hidden variable is calculated in such a way that it maximizes the amount of variation explained among response variables. The second hidden variable maximizes the amount of variation left after the first hidden variable. The consecutive hidden variables are

calculated is similar way. The requirement is that all hidden variables must be orthogonal to each other. PLS model parameters comprise weight vectors that are used to build hidden variables from original variables, and loading vectors that are used to produce predicted values of response variables from hidden variables.

As the number of hidden variables increases the accuracy of PLS model approaches accuracy of OLS model but it will not produce better results. Typically first few hidden variables explain about 90% of variation among data and only these are used to build model. Worse performance of PLS model for training data used to build model might be compensated by better results produced by PLS model for test data. This follows from the fact that since OLS model finds the best fit of model parameters to training data it might lead to model overfitting. On the other hand PLS model adjusts model to training data only based on amount of variation that is explained by hidden variables. The amount of variation that can't be explained by hidden variables is ignored.

5. PLS model

As the input data for the model 6 control parameters of EB unit were taken: welding speed, beam current, frequency, accelerating voltage, beam focus distance from workpiece surface, and beam deflection. Additionally beam focus parameter was split into 2 separate parameters: one that takes values of beam focus if they are positive and otherwise is equal to 0, and the one that takes values of beam focus if they are negative and otherwise is equal to 0. The motivation for the split is that the character of dependency between beam focus distance and FZ geometry is different for cases corresponding to beam focus above workpiece surface and different for cases corresponding to beam focus below workpiece surface.

PLS model assumes that dependencies in data are linear. Since the actual dependencies are best described by quadratic polynomial input data were pre-processed. Second order polynomial dependency described as $f(x) = ax^2+bx+c$ was changed to linear dependency $f(x_1, x_2)= ax_1+bx_2+c$, where $x_1=x^2$ and $x_2=x$. Thus for each of input parameters new one was created which is equal to the square of the original one. Finally 14 parameters were used as input to PLS model.

The input data comprise 49 welds divided into 7 series. Welds were created for plate of depth equal to 14 mm. One reference set of EB unit control parameters was selected, Table 1. Subsequently for each series only one of the control parameters was modified. For beam focus parameter one series was performed for beam focus

above workpiece surface and one series for beam focus below worpiece surface.

Reference set of EBW parameters

voltage (kV)	current (mA)	speed (mm/s)	focus (mm)	oscillation (HZ)	deflection
120	20	20	0	800	0.15

Two separate PLS models were created, one for FZ depth and one for FZ width. PLS model for FZ depth used first 4 hidden variables that account for 94.2% of variation among response data and PLS model for FZ width used also first 4 hidden variables that account for 91.9% of variation among response data. Comparison of actual values and predicted values for FZ depth and width is shown in Fig. 1 and 2 respectively. Distance from a point to the reference line in vertical direction represents the error introduced by PLS model.
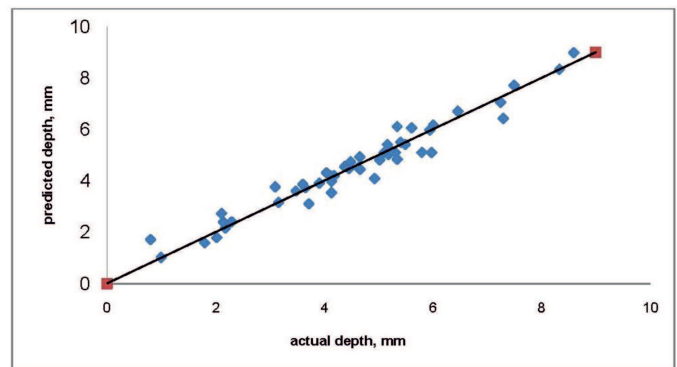

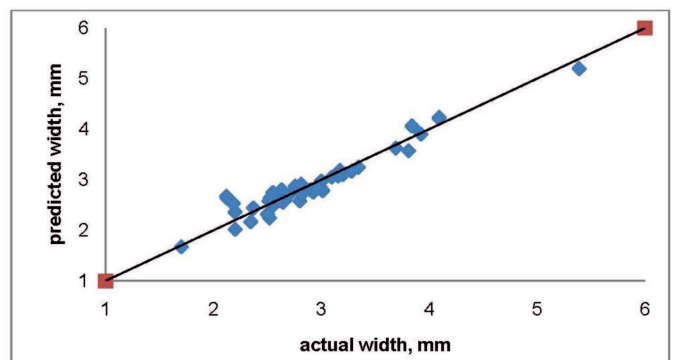Fig. 1. Comparison of actual and PLS predicted FZ depth

Fig. 2. Comparison of actual and PLS predicted FZ width

For comparative purposes OLS model was built using the same variables. As expected for training data it calculated results with better accuracy. Sum of squared

458

errors of predictions, SSE, was used as a measure of accuracy. It is defined as:

$$SSE = \sum_{i=1}^{n} (y_i - \hat{y}_i)^2 \qquad (1)$$

where: y_i – actual value, $\hat{y}_i$ – value predicted by model. In case of FZ depth SSE for PLS and OLS model was 7.3 and 5.7 respectively. In case of FZ width SSE for PLS and OLS model was 1.5 and 1.3 respectively.

6. Application of PLS model to Inconel data

PLS model built using 18-8 steel training data was applied to the set of parameters reported by Ferro, workpiece 1 in Table 2. It can be seen that unlike in the case of training data accuracy of PLS model is better than accuracy of OLS model, Table 3. The error introduced by models can be explained by different physical properties of steel and Inconel, and by the fact that in the training data for the model only one parameter was changed in each case. During experiment made by Ferro several parameters were modified at once with respect to the reference set presented in Table 1.

Absolute values of weld pool dimensions for steel and Inconel are different however the character of process parameter impact on weld pool geometry is similar thus it was decided to assign to the Ferro's pool geometry similar geometry from the own research results. As a measure of similarity between pools the ratio of depth to width was used. Once the similar geometry

and the corresponding process parameter set were identified PLS model was used to identify the impact of single parameter change on the depth of pool. Beam current was selected as the parameter that will be modified.

The ratio of depth (6.2) to width (3.4) for the Ferro's pool geometry is 1.82. The pool geometry with ratio 1.85 was selected as the similar pool. Target depth of weld pool is 5mm. The parameters reported by Ferro must be modified to produce fusion zone of depth equal to 81% of the original depth. According to PLS model reduction of current for the selected pool to 84% results in decrease of depth to 81% and decrease of width to 93%. Thus in Ferro's set of parameters value of current should be reduced to 8.4 mA to produce depth of 5mm.

7. FEM model

FEM was used to simulate thermal and stress field during welding process. The analysis was performed using program ADINA. Thermal field was described using Fourier-Kirchoff equation:

$$\frac{\partial T}{\partial t} = a\nabla^2 T + \frac{q_v}{\rho c_p} \qquad (2)$$

where: a – thermal diffusivity, ρ – density, c_p – specific heat, q_v – efficiency of inner volume heat source. Thermo-mechanical coupled, TMC, analysis was used to determine the magnitude of thermal stresses. Thermal elasto-plastic material model was assumed in the numerical model.

TABLE 2

EBW parameters and pool geometry for Inconel 706 plate, based on [5]

workpiece id	voltage (kV)	current (mA)	speed (mm/s)	focus (mm)	oscillation (Hz)	deflection	depth (mm)	width (mm)
1	150	10	10	+2	0	0	6.2	3.4
2	150	15	10	-20	0	0	5.7	4.5

TABLE 3

Comparison of PLS and OLS model results for FZ depth

Experimental (mm)	PLS model (mm)	PLS introduced error	OLS model (mm)	OLS introduced error
6.2	5.62	-9.4%	4.32	-30,3%
5.7	6.19	8.6%	4.86	-14.7%

Three-dimensional heat source model was applied for the purpose of simulation. The nail shaped heat source in transverse direction reflects FZ specific to EBW. The elongated shape of heat source in longitudinal direction represents movement of heat source. Heat source is built from hexahedron elements. Its shape is defined by 4 points which correspond to depth, width, and the shape of 'nail head', Fig. 3. The model assumes uniform power distribution. The motion of electron beam along welding trajectory is represented by production of heat in consecutive heat source volumes. At any time heat is produced only in one heat source volume. The number of heat source volumes is defined as quotient of weld trajectory length and heat source length.

The important parameter in the simulation of welding processes is power absorption coefficient which represents the actual amount of power absorbed by material during welding process. The actual cross-section dimensions of FZ were used to calibrate FEM model. It is assumed that if the size and shape of actual FZ is consistent with values calculated by FEM model then temperatures calculated outside FZ are also correct. This follows from the fact that heat flow in transverse direction dominates in welding [9]. Fig. 4 presents microstructure of weld produced by Ferro and results of own numerical simulation which are represented by isotherms. In order to achieve consistency of actual and predicted FZ power absorption coefficient was set to η=57%.

Process parameters and geometry calculated by PLS model, and power absorption coefficient obtained during heat input calibration were used to define target FEM model of tube welding. Heat source power was set to $\eta \cdot$ 150000V $\cdot$ 0.0084A = 718.2W. Heat source depth was set to 5mm and heat source width was set to 3.2mm. Welding time was set to 10.21 s so that welding speed is equal to 10 mm/s. Heat source volume count was set to 36. Thus duration of heat input corresponding to single heat source volume is 0.28s.

Fig. 5 presents the results of thermal analysis for target FEM. Fig. 5 (a) presents temperature distribution for time corresponding to maximal size of fusion zone. The maximal temperature predicted by model is 2390°C degrees. Fig. 5 (b) presents size of fusion zone. It can be seen that fusion depth is enough to join 2 tubes. The shape of fusion zone reflects the actual 'nail-shaped' fusion zone typical for EBW in deep penetration mode.

Fig. 6 presents distribution of stress in joint cross-section. Fig. 6 (a) shows stress field at cross section of first heat source volume at time 0.28s corresponding to maximal heat input received. It can be seen that region of lowest stress values corresponds to the area of molten metal. High values of stress occur around FZ. The highest stress values occur at the inner wall tube and equal about 300MPa. Fig. 6 (b) presents stress field at the same cross section at time 0.56s. As temperature decreases stresses in the area corresponding to weld pool start to grow. The highest value of stress drops to about 240MPa.
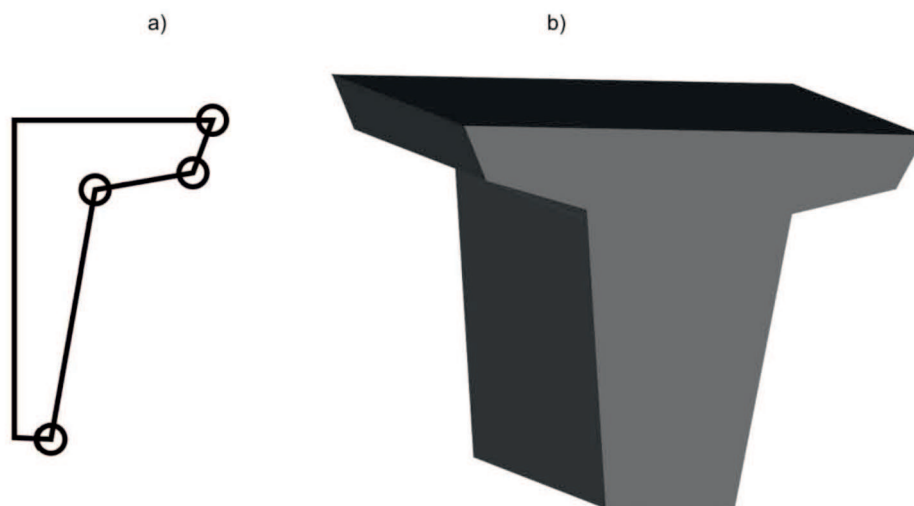

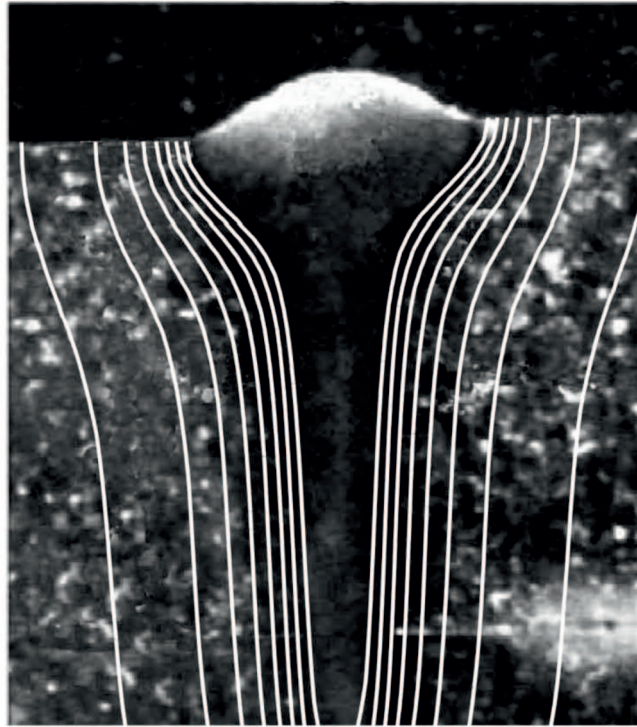Fig. 3. Heat source model (a) 2D view (b) 3D view

Fig. 4. Microstructure of Inconel 706 weld based on [5] and isotherms representing results of own numerical simulation. Isotherm closest to FZ represents temperature 1350°C and consecutive isotherms decrease by 180°C
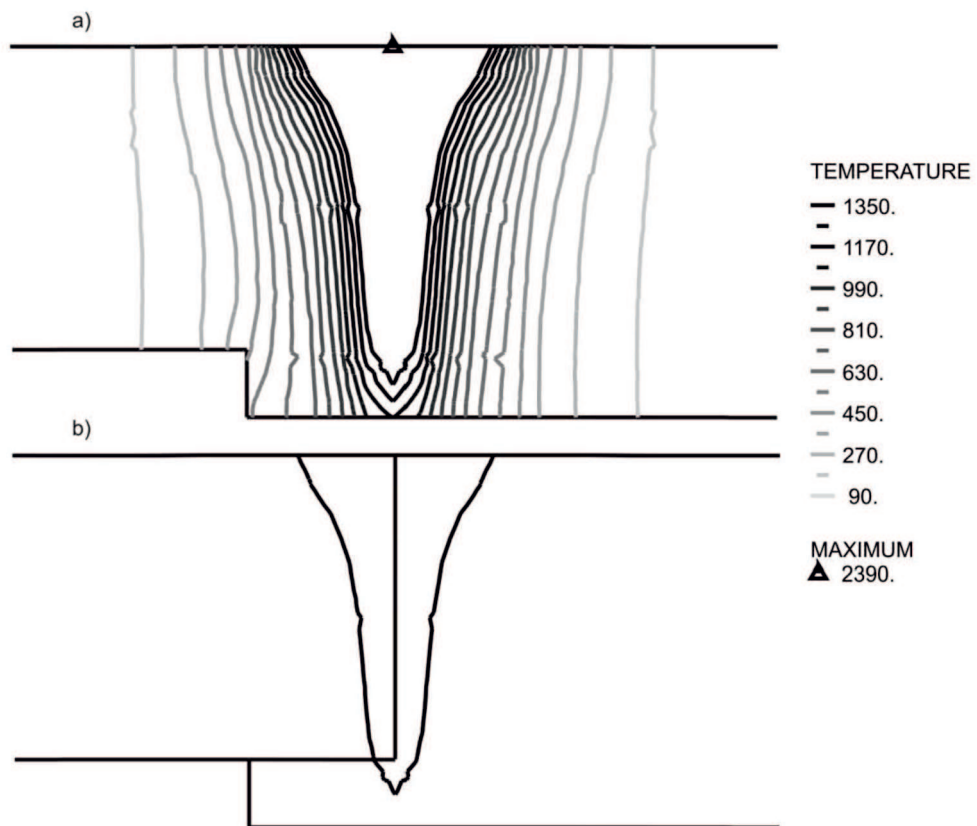

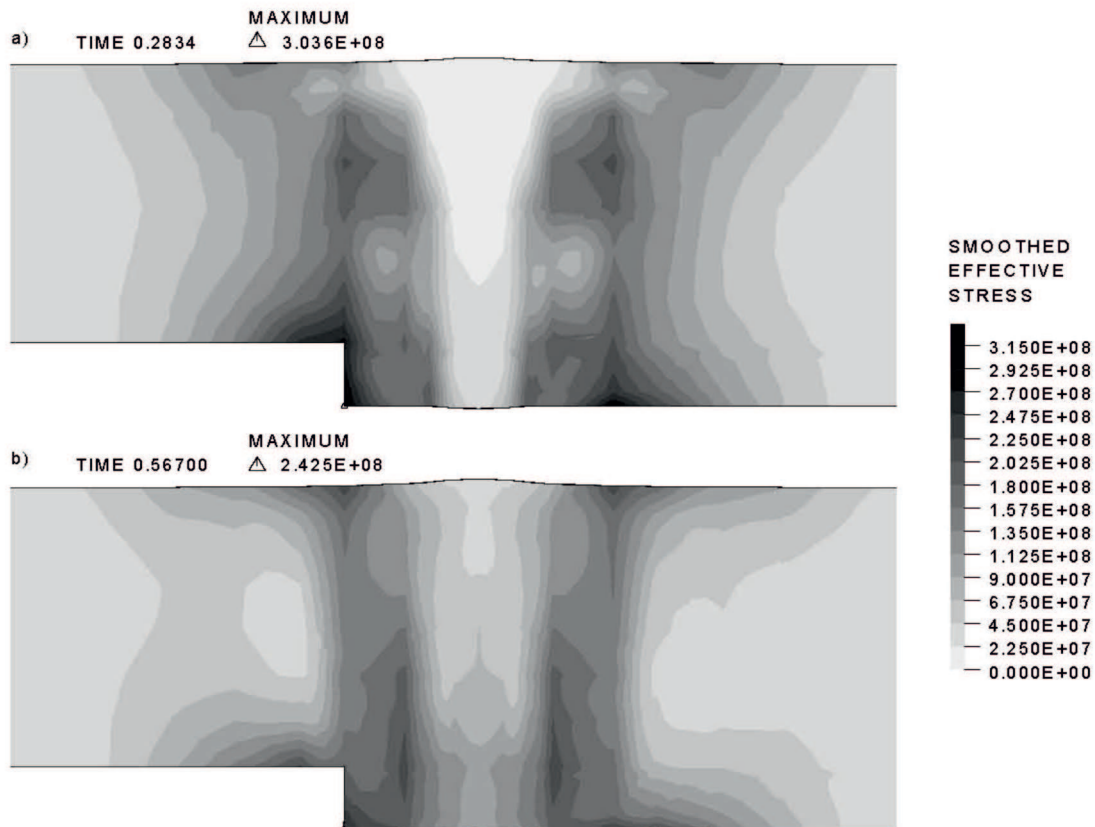Fig. 5. (a) temperature distribution during EBW process (b) FZ and schematic view of joint

Fig. 6. Effective stress distribution during EBW process at time: (a) 0.28s (b) 0.56s

8. Conclusions

In the paper the extension of FEM modeling of welding process with PLS method was suggested. Key aspect of welding process analysis using FEM is specification of power field which has direct impact on dimensions of FZ. Frequently one of the requirements during welding is to achieve the specified penetration of weld. FEM alone doesn't indicate the depth of FZ based on welding process heat input. PLS method helps to identify dependency between welding process parameters and dimensions of FZ. The calculated dimensions of FZ can be applied to definition of power field in FEM.

PLS method was compared to OLS method. It was shown that while OLS method gives better results for training data PLS might be more accurate for test data. This can be explained by the fact that PLS method only captures information that is well explained by independent variables.

REFERENCES

[1] H. Z a t y k a, Spawanie wiązką elektronów, WNT, Warszawa, 1968.

[2] H. S c h u l t z, Elektronenstrahlschweißen, DVS, Düsseldorf, 2000.

[3] Technical bulletin: Inconel alloy 706 (Publication number SMC-091), Special Metals Corporation (http://www.specialmetals.com), September 2004.

[4] A.T. E g b e w a n d e, R.A. B u c k s o n, O.A. O j o, Analysis of laser beam weldability of Inconel 738 superalloy, Materials characterization, 61 569-574 (2010).

[5] P. F e r r o, A. Z a m b o n, F. B o n o l l o, Investigation of electron beam welding in wrought Inconel 706 – experimental and numerical analysis, Materials Science and Engineering A **392**, 94-105 (2005).

[6] G. M a d h u s u d h a n a R e d d y, C. V. S r i n i - v a s a M u r t h y, K. S r i n i v a s a R a o, Prasad Rao K., Improvement of mechanical properties of Inconel 718 electron beam welds–influence of welding techniques and postweld heat treatment, The Internation-

462

al Journal of Advanced Manufacturing Technology **43**, 671-680 (2009).

[7] H. Y a n g, Y. C a i, Y. B a o, Y. Z h o u, Analysis and application of partial least square regression in arc welding process, Journal of Central South University of Technology **12**, 453-458 (2005).

[8] V. E s p o s i t o V i n z i, W.W. C h i n, J. H e n s l e r, H. W a n g, Handbook of partial least squares. Concepts, methods and applications, Springer, 2010.

[9] L.E. L i n d g r e n, Computational welding mechanics. Thermomechanical and microstructural simulations, Woodhead Publishing, Cambridge, 2007.